How Cr changes the dislocation core structure of α-Fe: the role of magnetism

2013 J. Phys.: Condens. Matter 25 085403

(http://iopscience.iop.org/0953-8984/25/8/085403)

IOP PUBLISHING JOURNAL OF PHYSICS: CONDENSED MATTER

J. Phys.: Condens. Matter **25** (2013) 085403 (5pp) doi:10.1088/0953-8984/25/8/085403

How Cr changes the dislocation core structure of α-Fe: the role of magnetism

Xu Zhang and Gang Lu

Department of Physics and Astronomy, California State University Northridge, Northridge, CA 91330-8268, USA

E-mail: ganglu@csun.edu

Received 18 September 2012, in final form 9 January 2013
Published 30 January 2013
Online at stacks.iop.org/JPhysCM/25/085403

Abstract

Cr is a critical alloying element in ferritic steels and its effect on the dislocation core structure of α-Fe is examined computationally using a quantum mechanics/molecular mechanics method. We find that Cr can significantly change the dislocation core structure of Fe where magnetism plays a crucial role. The strain-dependent magnetic interaction between Cr and the host Fe atoms is responsible for the dislocation core structure. When Cr is at the tension side of the slip plane, the Cr–Fe magnetic interaction is repulsive, which lowers the dislocation energy and pins the dislocation. When Cr occupies the compression side of the slip plane, the Cr–Fe interaction is attractive which increases the dislocation energy and promotes the dislocation to break away from Cr.

(Some figures may appear in colour only in the online journal)

1. Introduction

Ferritic steels are prime candidates for structural components of fusion reactors, in which Cr is a critical alloying element contributing to improving the materials' resistance to corrosion, irradiation and swelling [1–3]. Understanding how Cr influences the mechanical properties of the ferritic steels represents a key challenge in designing the next generation nuclear reactors. Hence a fundamental understanding of how Cr changes the dislocation core properties of α-Fe is of both scientific importance and technological relevance. It has been recently demonstrated that magnetism could play an important role in the mechanical properties of materials, establishing a connection between the two disparate fields [5, 4]. For example, it was discovered experimentally that 3d transition metal impurities such as Fe, Co, Ni, Cr, could profoundly change the mechanical strengths of B2-NiAl intermetallic alloys; the origin of the impurity-induced solid solution *softening* in these alloys was attributed to the magnetic interaction between the impurities and the host atoms [5]. Zhao *et al* [6] have carried out first-principles simulations to understand the interplay between magnetism and dislocation core properties in NiAl alloys. They observed magnetism-driven site preference of the impurities at the dislocation core, and depending on the occupation sites, the impurities can either promote spontaneous dislocation cross-slip or render the dissociation of a complete dislocation into partials. More importantly, the simulations revealed magnetism-driven dislocation mobility, which is consistent with the experimental findings. Although it has been recognized that the magnetic interaction between the impurities and the host atoms is responsible for the significant changes to the dislocation core structure and mobility, a fundamental understanding of this magnetic interaction is still lacking. In this paper, we study the effect of Cr impurity on the core structure of an edge dislocation in α-Fe and observe dramatically different dislocation core structures with Cr at the opposite sides of the slip plane. We attribute the disparate core structures to *strain-dependent* magnetic interaction between Cr and Fe; the opposite strains across the slip plane give rise to the opposite Cr–Fe magnetic interactions, which ultimately lead to different dislocation core structures and mobilities.

Previously, atomistic simulations using empirical interatomic potentials have been performed to examine the effect of Cr on the dislocation properties of Fe [7–10]. Unfortunately, the delicate magnetic interaction between Cr and Fe cannot be captured accurately by the empirical potentials. On the other hand, although quantum mechanical (QM) simulations are capable of describing the magnetic interaction, they are often computationally too expensive to deal with dislocations. Thus computational algorithms that combine quantum mechanics with molecular mechanics (QM/MM) emerge as a promising solution to the challenge.

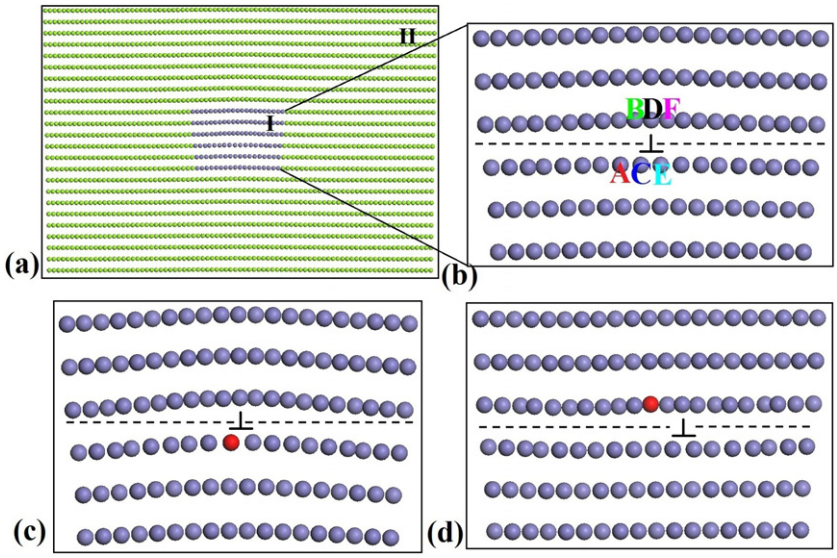

Figure 1. (a) Partition of the entire system into region I (blue spheres) and region II (green spheres, partially shown). (b) Atomic structure of region I for the edge dislocation in α-Fe. Selective atoms at the dislocation core are labeled from A to F; D is at the center of the dislocation core. Dislocation structure with a Cr impurity occupying at (c) the C site and (d) the D site. The red spheres represent the Cr atom and the inverted 'T' symbol denotes the center of the dislocation. The dashed line indicates the slip plane.

However, as demonstrated in this paper, existing QM/MM methods based on QM cluster calculations actually fail to yield the correct dislocation core structure in Fe and the failure is due to the incorrect magnetic moments at the cluster surface. To circumvent this problem, we employ a newly developed QM/MM method based on constrained density functional theory (DFT), which eliminates the errors in magnetic moments and provides an accurate description of the dislocation core structure in Fe.

2. Method and computational models

In the QM/MM approach, the entire modeled system is partitioned into two spatial domains: a QM region treated by DFT and a MM region by empirical atomistic simulations. The QM region is further divided into an interior QM region and a boundary QM region. The former involves bond breaking, chemical reaction and charge transfer, etc where topological changes of charge density take place. The latter serves as a buffer region where no such topological change to the charge density occurs. The MM atoms interact *directly* with the boundary QM atoms but only indirectly with the interior QM atoms; on the other hand, the interior QM atoms interact directly with the boundary QM atoms and its interaction energy is formulated based on the constrained DFT [11–13]. In other words, the boundary QM region serves both as a buffer (the interior QM atoms do not interact the MM atoms directly) and a bridge between the interior QM region and the MM region. The total energy of the QM/MM system can be expressed as

$$E_{\rm tot} = E^{\rm DFT}[\rho_{\rm QM}; \mathbf{R}_{\rm QM}] - E^{\rm MM}[\rho^{\rm b}_{\rm QM}; \mathbf{R}^{\rm b}_{\rm QM}] + E^{\rm MM}[\mathbf{R}^{\rm b}_{\rm QM} \cup \mathbf{R}_{\rm MM}], \quad (1)$$

where the first term denotes the energy of the full QM region calculated via the constrained DFT. The last two terms are the energy of the QM boundary region and the combined QM boundary/MM region, respectively as determined by the empirical MM simulations. The last term is the energy of the combined QM boundary/MM region as determined by the empirical MM simulations. $\mathbf{R}_{\rm QM}$, $\mathbf{R}^{\rm b}_{\rm QM}$ and $\mathbf{R}_{\rm MM}$ represent atomic coordinates in the full QM, the QM boundary and the MM regions, respectively. $\rho_{\rm QM}$ and $\rho^{\rm b}_{\rm QM}$ indicate the corresponding charge densities. Since there is no topological change to $\rho^{\rm b}_{\rm QM}$, it should be bulk-like and thus can be well represented by a superposition of 'atomic' charge densities, determined *a priori* for each ionic species. As a key component of the QM/MM method, the constrained DFT allows a self-consistent determination of $\rho_{\rm QM}$ by constraining $\rho_{\rm QM}$ to a pre-determined charge density *in the boundary region*. The essence of the QM/MM method is to ensure that the QM region is treated in the presence of appropriate boundary conditions provided by the charge density and potentials of the MM atoms; this is in stark contrast to other QM/MM methods where the QM region is treated as a bare cluster. The technical details and validations of the QM/MM method can be found elsewhere [14].

As shown in figure 1, the entire dislocation system includes two regions. The QM region (region I) contains the dislocation core with/without a Cr impurity; the MM region (region II) consists of the rest of the system including the long-range elastic field of the dislocation. The edge dislocation in α-Fe has a Burgers vector of $\mathbf{b} = \frac{1}{2}\langle 111\rangle$ on the $\{110\}$ slip plane. The entire QM/MM system measures 202 Å × 202 Å × 6.93 Å in [111], $[\bar{1}10]$, and $[\bar{1}\bar{1}2]$ directions, respectively, with 25 398 atoms in total. Fixed boundary conditions are applied along [111] and $[\bar{1}10]$ directions with the boundary displacement field determined by the isotropic elastic solution of the dislocation. The dislocation line is

along the $[\bar{1}\bar{1}2]$ direction in which the periodical boundary conditions are applied. The dimensions of region I are 21 Å × 10 Å × 6.93 Å with 153 atoms, and the rest of the system belongs to region II. The dislocation core is initially placed at the center of region I as displayed in figure 1(b). We have considered two substitutional sites for the Cr impurity at the dislocation core: one is at the tension site below the slip plane as shown in figure 1(c) and the other is at the compression site above the slip plane as depicted in figure 1(d). The Cr atoms are separated by 6.93 Å in the z direction which is large enough to eliminate chemical interaction between them.

The DFT calculations are performed using the VASP package [15, 16] with the projector augmented wave pseudopotentials [17] and Perdew–Burke–Ernzerhof generalized gradient approximation (PBE-GGA) [18]. An energy cutoff of 300 eV is used for the plane-wave basis set, and the k-point sampling is based on the Monkhorst–Pack scheme [19] with a $1 \times 1 \times 5$ mesh. The embedded atom method (EAM) [20, 21] of Fe is used in the MM simulations. The atomic relaxation is carried out with the conjugate-gradient algorithm and the force convergence criterion is 0.04 eV Å^{-1}.

3. Results and discussion

We find that the Cr impurity significantly changes the dislocation core structure of α-Fe. When Cr occupies the C site at the tension side, the dislocation core structure bends upward and the Cr atom pushes apart the neighboring Fe atoms to make room for itself as shown in figure 1(c). The total energy difference between Cr at the C site and the A site is 0.1 eV, suggesting an energy barrier of 0.1 eV for the dislocation to break away from the Cr impurity at the C site. Therefore the dislocation is pinned by the Cr impurity at the tension side of the slip plane. When Cr occupies the D site at the compression side, a spontaneous dislocation glide occurs and the dislocation core translates about $\frac{2}{3}\mathbf{b}$ away from the impurity as illustrated in figure 1(d).

To understand the effect of Cr on the dislocation core structure, we examine the nearest neighbor Cr–Fe atomic forces in equilibrium and under compression (with −7% strain) and tension (7% strain) strains. The ±7% strain corresponds to the local strain value at the dislocation core above and below the slip plane. The strained bcc lattice is modeled by a $5a_0 \times 5a_0 \times a_0$ supercell with the Cr impurity placed at the center. Here a_0 is the lattice constant of the bcc-Fe and is varied to simulate the volumetric strain. The periodic DFT calculations are performed to determine the atomic forces of the unrelaxed lattice, which are shown in figure 2. We find that the nearest neighbor Cr–Fe atomic force is attractive for the lattice in equilibrium and in compression, while the atomic force is repulsive for the lattice in tension. Moreover, the force changes the direction at ∼3% tension. However, in the spin-off DFT calculations, the nearest neighbor Cr–Fe force stays attractive irrespective of the strain. Therefore, we conclude that the alternating Cr–Fe atomic force is the result of magnetic (exchange) interaction between the atoms (spins) and this interaction depends sensitively on the local strain. Note that although the atomic radius of Cr is slightly larger (0.1 Å) than that of Fe, the atomic forces on the nearest neighbor Fe atoms are nonetheless attractive as shown in figure 2(b). This suggests that the size effect of the impurity is negligible whereas the electronic/magnetic interaction is dominant in this material.

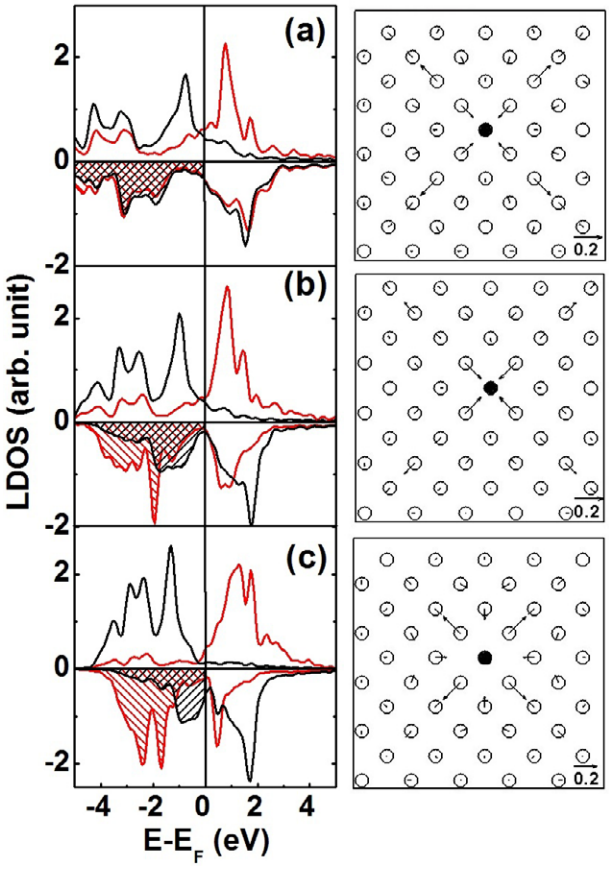

Figure 2. The partial DOS (left) and atomic force (right) in the bcc-Fe lattice under (a) compression, (b) equilibrium, and (c) tension with a substitutional Cr atom. The red and black curves denote the partial DOS of the Cr impurity and its nearest neighbor Fe atom, respectively. The positive (negative) values of DOS are presented for the spin-up (down) states. The shaded area represents the overlap in DOS between Cr and Fe atoms. The filled and empty circles represent Cr and Fe atoms, respectively. The unit of the atomic force is eV Å^{-1}.

In table 1, we present the magnetic moment on Cr and Fe under different strain conditions. First, Cr maintains antiferromagnetic interaction [22, 23] with its nearest neighbor Fe atoms irrespective of strain. Second, in the presence of Cr, the magnetic moment on the nearest neighbor Fe is lowered slightly by ∼0.1 μ_B. Third, as the strain increases from compression to tension, the magnetic moment on both Fe and Cr increases correspondingly. The interplay between magnetism and strain can be revealed from the d-band density of states (DOS) shown in figure 2. Owing to the antiferromagnetic interaction between Cr and Fe, the spin-up states correspond to the majority spin on Fe and the minority spin on Cr, while the spin-down states refer to the minority spin on Fe and the majority spin on Cr. As strain is increased from compression (figure 2(a)), to equilibrium (figure 2(b)) and to tension (figure 2(c)), the occupied majority

Table 1. Magnetic moment (in μ_B) on the Cr atom μ_{Cr}, its nearest neighbor Fe atom $\mu_{Fe(nn)}$ and the Fe atom farther away from Cr $\mu_{Fe(pure)}$ in compression, equilibrium and tension. The substitutional energy E_{sub} (in eV) is calculated as the cohesive energy difference in the presence and absence of the Cr impurity; a more negative E_{sub} indicates that the substitution is energetically more favorable.

	μ_{Cr}	$\mu_{Fe(nn)}$	$\mu_{Fe(pure)}$	E_{sub}
Compression	−0.39	1.63	1.76	−0.92
Equilibrium	−1.51	2.14	2.19	−1.22
Tension	−3.02	2.59	2.69	−1.30

DOS for both Fe and Cr increases whereas the minority DOS decreases. This explains the results shown in table 1 where the magnetic moment on Fe and Cr increases with increasing strain. Since the states below the Fermi energy contribute to the electron bonding, the overlap between the minority d-DOS of Fe (the negative black curve) and the majority d-DOS of Cr (the negative red curve) is primarily responsible for Cr–Fe bonding; this is indicated by the shaded areas in figure 2. With increasing strain, the Fe minority d-band shifts towards the Fermi energy while the Cr majority d-band remains nearly in the same position. As a result, the two d bands decouple and the shaded area shrinks with increasing strain as shown in figure 2. This decoupling of the d-bonding states weakens Fe–Cr bonding, and leads to the transition of Fe–Cr interaction from attractive to repulsive with increasing strain.

The influence of Cr on the dislocation core structure can be rationalized by considering the changes of the dislocation misfit or γ-energy and the substitutional energy of Cr; both of them depend on the magnetic Cr–Fe interaction. We calculate the γ-energy along the $\langle 111 \rangle$ direction for Fe with and without Cr as shown in figure 3. The γ-energy on the {110} slip plane is determined by using a supercell consisting of eight (110) atomic layers [24]. The unstable stacking fault energy of 61 meV Å^{-2} for pure Fe agrees well with other DFT results [25, 26], which is slightly increased by 2 meV Å^{-2} in the presence of Cr. The displacement field of the edge dislocation is also presented in figure 3. As shown in table 1, Cr prefers to occupy the sites on the tension side of the slip plane. When Cr occupies the C site in tension, the γ-energy is lowered as indicated in figure 3(b) because the neighboring Fe atoms on the positions A and E are pushed away from C due to the repulsive Cr–Fe interaction. In addition, the occupation of the site C is also preferred from the substitutional energy perspective. Therefore, overall it is energetically favorable for Cr to occupy the tension side of the slip plane. If the dislocation breaks away from the Cr atom, the local strain at the site C will decrease. The decreasing strain has two consequences: (1) it would act against the repulsive Cr–Fe interaction and thus increase the bonding energy; (2) it would increase the substitutional energy. Consequently, the dislocation energy would increase if the dislocation breaks away from Cr at the C site. In other words, the Cr atom at the C site would pin the dislocation. On the contrary, when Cr occupies the D site on the compression side, the Fe atoms on the B and F sites are attracted to Cr due to the attractive Cr–Fe

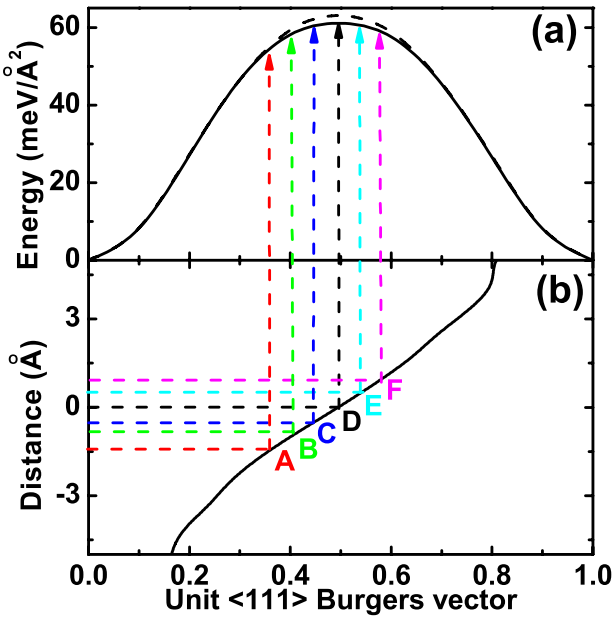

Figure 3. (a) The γ-energy of pure Fe (solid curve) and Fe with a substitutional Cr atom (dashed curve). (b) The edge component of the displacement field is in units of the Burgers vector, and zero indicates the center (at the D site) of the dislocation.

interaction in the compression region, which increases the γ-energy. At the same time, the substitutional energy is also increased in the compression region. Therefore the dislocation tends to break away from Cr at the compression sites to lower its energy.

Finally, we address the importance of the present QM/MM method in dealing with magnetic systems. A majority of existing QM/MM methods are based on the so-called mechanical coupling scheme which involves cluster calculations of the QM region [27, 28]. Unfortunately, such cluster calculations can lead to significant errors of magnetic moment at the surface of the cluster, as illustrated in figure 4(a). Because of the errors at the QM/MM boundary, the dislocation core experiences a fictitious force which prevents it from breaking away from Cr at the D site. This is in contradiction to the result obtained by the present QM/MM method. To understand the contradiction, we consider the Peierls–Nabarro model of dislocations in which the equilibrium dislocation structure is determined by a balance between a repulsive elastic stress among infinitesimal dislocations and an attractive restoring stress [24]. The former depends on the elastic moduli of the material while the latter can be determined from the gradient of the γ-energy. We have calculated the restoring stress as a function of displacement for two model systems. In each system, the magnetic moment on ions is fixed at a certain value. The first system has a magnetic moment of 2.2 μ_B on each ion which is the same as that of bulk bcc-Fe; the second system has a magnetic moment of 2.9 μ_B on each ion which is the same as that at the cluster surface. We find that both the γ-energy and the restoring stress for the first system are greater than those of the second system, as shown in figures 4(b) and (c). The different γ-energy and the restoring stress will yield

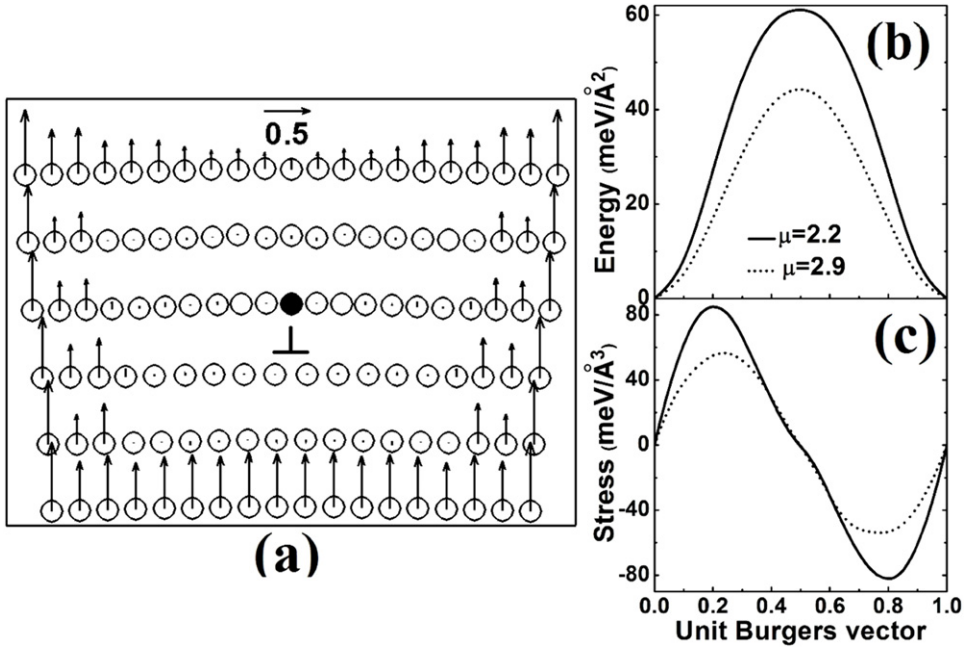

Figure 4. (a) The atomic structure of the dislocation with Cr at the D site determined by the mechanical coupling QM/MM method. The arrows denote the magnetic moment difference obtained by the DFT cluster calculation of the region I and the present QM/MM simulation. The γ-energy (b) and restoring stress (c) calculated by DFT with μ_{Fe} of 2.2 and 2.9 μ_{B}.

drastically different dislocation core structures, as discussed above. Because the present QM/MM method can eliminate the errors of magnetic moment at the cluster surface [14], it can provide a much more accurate description of dislocation core structure in magnetic materials.

4. Conclusion

In summary, we have studied the effect of Cr impurity on the dislocation core properties of α-Fe using a novel QM/MM method. We found that Cr can substantially change the dislocation core structure driven by the magnetic interaction between Cr and Fe. The strain-dependent magnetic interaction is responsible for the changes in the dislocation core structure. When Cr occupies the tension side of the slip plane, the Cr–Fe interaction is repulsive which lowers the dislocation energy and pins the dislocation. When Cr is at the compression side of the slip plane, the Cr–Fe interaction is attractive which increases the dislocation energy and promotes the dislocation to break away from Cr. Finally, we show that the present QM/MM method provides a more accurate description of magnetic materials than other QM/MM methods.

Acknowledgment

This work was supported by the Office of Naval Research.

References

[1] Klueh R L, Ehrlich K and Abe F 1992 *J. Nucl. Mater.* **191** 116
[2] van der Schaaf B, Gelles D S, Jitsukawa S, Kimura A, Klueh R L, Mosloang A and Odette G R 2000 *J. Nucl. Mater.* **283** 52
[3] Malerba L, Caro A and Wallenius J 2008 *J. Nucl. Mater.* **382** 112
[4] Liu C T, Fu C L, Pike L M and Easton D S 2002 *Acta Mater.* **50** 3205
[5] Liu C T, Fu C L, Chisholm M F, Thompson J R, Krcmar M and Wang X L 2007 *Prog. Mater. Sci.* **52** 352
[6] Zhao Y, Wang C and Lu G 2010 *Phys. Rev.* B **82** 060404(R)
[7] Farkas D, Schon C G, DeLima M S F and Goldenstein H 1996 *Acta Mater.* **44** 409
[8] Hafez Haghighat S M, Terentyev D and Schaublin R 2011 *J. Nucl. Mater.* **417** 1094
[9] Terentyev D, Bonny G, Domain C and Pasianot R C 2010 *Phys. Rev.* B **81** 214106
[10] Chen Z, Kioussis N, Ghoniem N and Hasebe T 2008 *Phys. Rev.* B **77** 014103
[11] Zhao Q and Parr R G 1992 *J. Chem. Phys.* **98** 543
[12] Zhao Q, Morrison R C and Parr R G 1994 *Phys. Rev.* A **50** 2138
[13] Wu Q and Van Voorhis T 2005 *Phys. Rev.* A **72** 024502
[14] Zhang X, Lu G and Curtin W A 2013 unpublished
[15] Kresse G and Hafner J 1993 *Phys. Rev.* B **47** 558
[16] Kresse G and Furthmuller J 1996 *Phys. Rev.* B **54** 11169
[17] Blochl P E 1994 *Phys. Rev.* B **50** 17953
[18] Perdew J P, Burke K and Ernzerhof M 1996 *Phys. Rev. Lett.* **77** 3865
[19] Monkhorst H J and Pack J D 1976 *Phys. Rev.* B **13** 5188
[20] Daw M S and Baskes M I 1984 *Phys. Rev.* B **29** 6443
[21] Shastry V and Farkas D 1996 *Simul. Mater. Sci. Eng.* **4** 473
[22] Lavrentiev M Y, Soulairol R, Fu C C, Nguyen-Manh D and Dudarev S L 2011 *Phys. Rev.* B **84** 144203
[23] Soulairol R, Fu C C and Barreteau C 2011 *Phys. Rev.* B **84** 155402
[24] Lu G, Kioussis N, Bulatov V V and Kaxiras E 2000 *Phys. Rev.* B **62** 3099
[25] Zhao Y and Lu G 2011 *Modelling Simul. Mater. Sci. Eng.* **19** 065004
[26] Ventelon L and Willaime F 2010 *Phil. Mag.* **90** 1063
[27] Gao J and Truhlar D G 2002 *Annu. Rev. Phys. Chem.* **53** 467
[28] Zhang X, Zhao Y and Lu G 2012 *Int. J. Multiscale Comput. Eng.* **10** 65